BIODIVERSITAS
Volume 26, Number 11, November 2025
Pages: 5770-5779

ISSN: 1412-033X
E-ISSN: 2085-4722
DOI: 10.13057/biodiv/d261135

Otolith morphometrics for growth and conservation assessment of endangered Napoleon wrasse (*Cheilinus undulatus*) in Sabah, Malaysia

EKO HENDRI GUNAWAN[1,2], CHING FUI FUI[1,♥], AUDREY DANING TUZAN[1], NAZIA ABDUL KADAR[1], FITTRIE MEYLLIANAWATY PRATIWY[3], IBNU DWI BUWONO[3], SHIGEHARU SENOO[1,4]

[1]Higher Institution Center of Excellence Borneo Marine Research Institute, Universiti Malaysia Sabah. Jl. UMS, 88400 Kota Kinabalu, Sabah, Malaysia. Tel.: +6088320000, ♥email: cfuifui@ums.edu.my

[2]Marine and Fisheries Quality Assurance Agency Cirebon, Ministry of Marine Affairs and Fisheries. Jl. Cideng Indah No. 236A, Cirebon 45153, West Java, Indonesia

[3]Aquaculture Department, Faculty of Fisheries and Marine Sciences, Universitas Padjadjaran. Jl. Raya Bandung Sumedang Km. 21, Sumedang 45363, West Java, Indonesia

[4]Aquaculture Technology and Production Center, Kindai University. Shirahama, Wakayama, 649-2211, Japan

Manuscript received: 21 August 2025. Revision accepted: 10 November 2025.

Abstract. *Gunawan EH, Fui CF, Tuzan AD, Kadar NA, Pratiwy FM, Buwono ID, Senoo S. 2025. Otolith morphometrics for growth and conservation assessment of endangered Napoleon wrasse (*Cheilinus undulatus*) in Sabah, Malaysia. Biodiversitas 26: 5770-5779.* The endangered Napoleon wrasse (*Cheilinus undulatus*) plays a vital role as a carnivorous fish in coral reef ecosystems. However, it faces severe threats from overfishing and habitat degradation, necessitating evidence-based conservation strategies. This study assessed growth pattern, biological condition, and size structure by integrating fish morphometric and otolith metrics from 41 specimens collected in Eastern Sabah, Malaysia. Fish total length from 27.51 to 103.88 cm (mean SD = 35.28±11.72 cm) and body weight from 330.24 to 19400.85 g (mean SD = 757.32±2934.41 g). Linear regression revealed a near-isometric length-weight relationship (b = 3.062, 95% CI [2.904, 3.219], r^2 = 0.975, $p<0.001$), indicating proportional growth with robust model fit. Fulton's condition factor (K) was stable across size classes (range: 1.319-2.089, mean ± SD: 1.695±0.189), showing no significant differences (ANOVA, $p>0.05$) and suggesting consistent physiological health amid environmental pressures. Size distribution was skewed toward juveniles and intermediates (<40 cm, 78% of samples), highlighting potential recruitment overexploitation. Otolith metrics demonstrated strong predictive power, with otolith weight correlating highly with fish length (r^2 = 0.784, $p<0.001$) and weight (r^2 = 0.766, $p<0.001$), validated through cross-validation (CV-MSE comparable to in-sample MSE) and residual diagnostics confirming normality, homoscedasticity, and independence. These findings highlight the vulnerability of *C. undulatus* populations in Eastern Sabah, which juvenile exploitation may undermine recovery potential. Otolith-based metrics provide cost-effective, essential baseline data for stock assessments, enabling precise monitoring of growth and demographics. For future conservation management, this supports implementation of minimum size limits, enhanced marine protected areas, and community-led surveillance, fostering sustainable recovery of this iconic species and reef biodiversity.

Keywords: Condition factor, coral reef fisheries, endangered species, length-weight relationship, sustainable management

INTRODUCTION

Napoleon wrasse (*Cheilinus undulatus* Rüppell, 1835) is a large and prominent reef predator integral to maintaining coral reef ecosystem balance by controlling populations of smaller fish and invertebrates (Roe et al. 2022). As a protogynous fish, it undergoes changes in gonadal development from female to male, which contributes to the population's complex dynamics. This biological trait renders the species vulnerable to exploitation (Ma et al. 2019). Globally, *C. undulatus* is listed as Endangered on the IUCN Red List due to overfishing, illegal trade, habitat degradation, and climate change, with population declining by over 50% in the past three decades (Vincent et al. 2022). In East Asian countries, particularly in high-demand markets such as Hong Kong and China, it is prized as a luxury seafood item and commands high prices, which incentivize unsustainable harvesting (Syam et al. 2020). Previous regional research conducted in Indonesia and the Philippines reveals a significant depletion of fish stocks, with juvenile-dominated catches suggesting overfishing of recruitment populations (Prianto et al. 2019; Nanola et al. 2021).

In the region of eastern Sabah in Malaysia, a biodiversity hotspot located within the coral triangle, *C. undulatus* is confronted with a multitude of threats that are compounded by destructive fishing practices, sedimentation resulting from coastal development, and climate-induced coral bleaching. Moreover, local investigation in Semporna District reveals fragmented habitat and reduced densities, exacerbating risks to reef resilience (Bavoh et al. 2023). Despite protections under CITES Appendix II and national regulations, enforcement challenges persist, leading to ongoing illegal trade. Consequently, the decrease in populations of *C. undulatus,* coupled with the degradation of its habitat, has raised significant concerns regarding the sustainability of coral reef fisheries and the overall health of marine biodiversity in Southeast Asia (Vincent et al. 2022).

Understanding growth patterns and population dynamics of *C. undulatus* is essential for effective management, yet data gaps remain, particularly with regard to wild populations in Sabah, where baseline metrics are severely limited (Tan et al. 2019). Morphometric analysis, including length-weight relationship (LWR) and condition factor (K), provides information on growth types, health, and environmental stressors (Jisr et al. 2018). Positive allometric growth reflects favorable conditions, while low K-values signal malnutrition or stress (Brosset et al. 2023). Otoliths, the calcareous structures of the inner ear of fish, provide valuable insight into the age and growth through their allometric relationship with size (Arancibia et al. 2021). Previous studies on other reef-associated fishes, such as blue fish (*Pomatomus saltatrix*) and flathead sillago (*Sillaginopsis panijus*), demonstrate strong correlations between otolith dimensions and somatic traits (De Souza et al. 2019; Pradhan et al. 2022). These data deliver insights into the growth and recruitment patterns of endangered species, thereby providing valuable information for conservation efforts (Rindorf et al. 2022). However, applications to *C. undulatus* remain scarce, with prior research focusing on captive populations (Tan et al. 2019) and not exploring otolith metrics, contrasting potential wild patterns. This gap is pronounced in Eastern Sabah, where overfishing targets large individuals, resulting in a skewed size structure favoring juveniles and impairing reproduction (Robinson et al. 2017).

Integrating fish morphometrics and otolith metrics could help enhance our understanding of the growth dynamics and fundamental population biology (Castro-Gutierre et al. 2023). This study provides the first otolith-based study of wild *C. undulatus* in Sabah. Specifically, this research seeks to determine the length-weight relationship (LWR) to characterize the growth pattern, assess the physiological well-being by using the condition factor (K), and establish the correlation between fish morphometric and otolith metrics to develop fish size predictive models. The hypotheses of this study are isometric or positive allometric growth in collected specimens, low K value due to various stressors, juvenile dominance from fishing pressure, and strong otolith correlation for reliable size prediction. Beyond advancing those fish biology attributes, the findings have broader implications for conservation strategies that involve community participation, size-based regulations, and habitat protection. Ultimately, this work provides foundational scientific data essential to address both biological vulnerabilities and socio-economic realities, ensuring long-term sustainability of this endangered species within the coral ecosystem in the region.

MATERIALS AND METHODS

Ethics and permits

All specimen collections complied with local fisheries regulations and conservation guidelines approval from Sabah Biodiversity Centre (SaBC) Permit No. JKM/MBS.1000-2/2JLD.21(85), Malaysia. Ethical approval for fish handling was granted by Universiti Malaysia Sabah Animal Ethics Committee (Approval code AEC 0009-2024), which stipulates minimal impact protocols for endangered species. Sampling was performed in accordance with animal welfare and biosecurity standards to minimize harm to this endangered species.

Specimen collection

Specimen collection was conducted with full consideration of its conservation status as a CITES Appendix II and IUCN-listed Endangered species. Consequently, field collection was restricted to opportunistic specimens obtained from licensed artisanal fishers operating in Semporna, Eastern Sabah, Malaysia (Latitude 4.4816° N, Longitude 118.6127° E) (Figure 1). All specimens were acquired using traditional hook-and-line fishing with range hooks sized 2/0-6/0. These ethical and regulatory constraints inevitably limited both the sample size (n = 41) and the temporal coverage (five sampling days in January 2025).

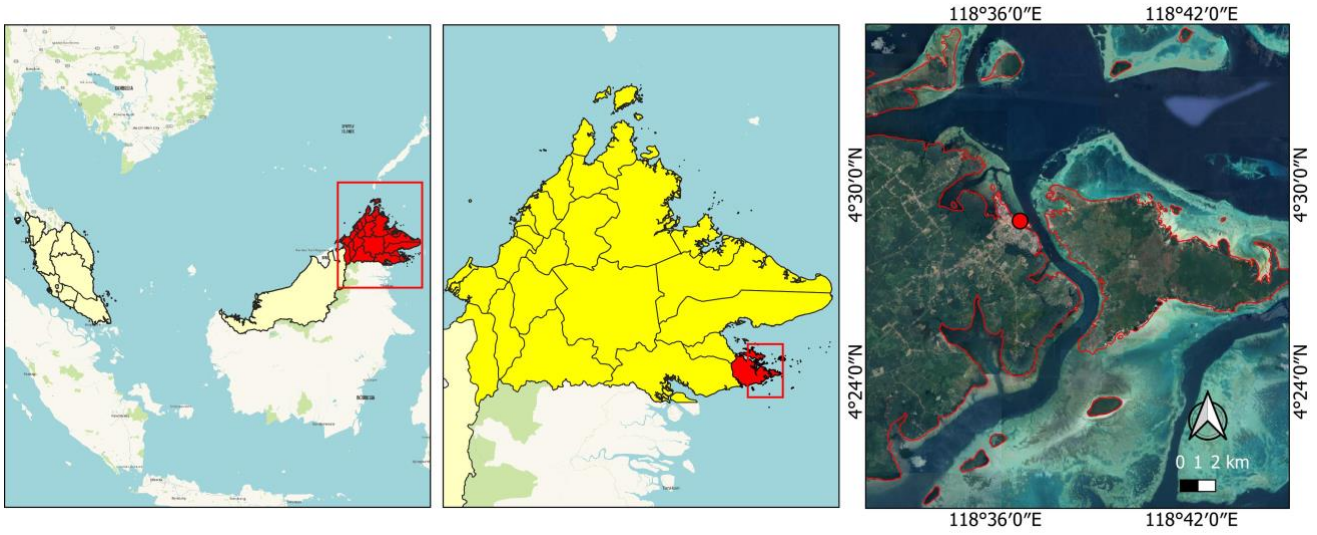

Figure 1. Map of sampling site in Semporna, Sabah, Malaysia

Morphometric measurements

Given the species' endangered status and limited access, the specimens collected represent the available size range of the population. This sample size is considered adequate as baseline data, following similar studies on rare reef fish where collection is restricted by regulations (n = 30-50) (Nanola et al. 2021). Sex determination through gonadal examination or dissection was not performed to avoid compromising the integrity of sampled individuals. All analyses were therefore conducted using pooled data irrespective of sex. This approach is enhanced by previous study, which stated that early life stages of *C. undulatus* exhibit minimal sexual dimorphism (Liu and Sadovy 2011). Each specimen was measured for fish total length (cm) using a measuring board and ImageJ v.1.53 software, calibrated to pixel-distance ratios specific to each image set, and fish body weight (g) using a digital scale (0.001 scale). These morphometrics were later used for assessing length-weight relationships (LWR) and condition factor (K).

Water quality parameters

In situ water quality measurements were taken at location to characterise the environmental conditions. The following parameters were measured using a calibrated multi-parameter probe (YSI ProDSS, USA): temperature, salinity, pH, dissolved oxygen (DO), brightness level, water depth, Total Dissolved Solid (TDS) and conductivity. The mean sea surface temperature was 27.3±0.10°C. Salinity averaged (34.963±0.02 ppt), reflecting oceanic conditions, while pH ranged between (7.79±0.14), indicative of slightly alkaline and stable seawater. Dissolved oxygen levels averaged (4.93±0.50 mg/L). The water depth and brightness level are 6.68 m and 4.42 m, respectively. Additional parameters showed Total Dissolved Solid (TDS; 34515 mg/L) and conductivity (55415±191.01 µS/cm), consistent with the ionic composition of offshore marine systems. Oxidation Reduction Potential ORP values (247.43±3.50 mV) indicated several marine pollutant parameters disturbances, such as organic matter build-up or lack of aeration.

Otolith extraction and measurement

Sagitta otoliths were extracted post-mortem by carefully removing gill arches, fracturing the skull to access the optic capsule, and retrieving otoliths with fine-tipped forceps to prevent structural damage. The extraction technique followed the procedure of De Souza et al. (2019) with minor adaptations. Otolith were rinsed, air-dried, and stored in labelled microtubes for subsequent measurements. Otolith length (OL; greatest anterior-posterior distance) and otolith height (OH; greatest dorsal-ventral distance) were measured using calibrated digital imaging system mounted on a Zeiss Discovery V8 stereomicroscope (Germany) with magnification x40 and resolution 0.001 mm. Otolith weight (OW) was recorded using a Precisa 404A analytical balance (Switzerland) accurate to 0.0001 g. To ensure consistency and minimize measurement bias, only the left sagitta were selected for analysis. Each observation under the microscope is carried out by two operators to minimize observer bias. In addition, subsequent regression analyses were then conducted on all otolith metrics against fish body length and weight, with the aim of evaluating morphometric relationships and potential predictive patterns. Representative otolith morphology is shown in Figure 2.

Data analysis and limitations

Data analysis

The length-weight relationship (LWR) was modelled using the power equation $W = aL^b$, W is body weight (g), L is total length (cm), (a) is the intercept, and (b) is the growth exponent (Abidin et al. 2019). A value of b>3 indicates positive allometric growth, while b<3 suggests negative allometry and b=3 indicates isometric growth. The relationship between total length (FL) and total weight (FW) is shown by coefficients of determination (r^2) (Jisr et al. 2018). Meanwhile, condition factor (K) was calculated by $K = \left(\frac{W}{L^3}\right) x100$ to assess the relative fish health and well-being of fish across size classes (Froese 2006). General linear models were applied to evaluate relationships between fish total length (FL)/weight (FW) and otolith dimensions (OL, OH, OW). The strength of their association was expressed as the coefficient of determination (r^2).

Normality and linearity assumptions were verified prior to analysis. In addition, collinearity diagnostic were also performed on the dataset. All statistical analyses were performed using IBM SPSS Statistics (Version 29.0.2.0) and Microsoft Excel (Version 16.89), with significance accepted at $p<0.05$ and confidence intervals (CI) set at 95%. Graphical outputs were used to visualize correlations, frequency distributions, and regression trends.

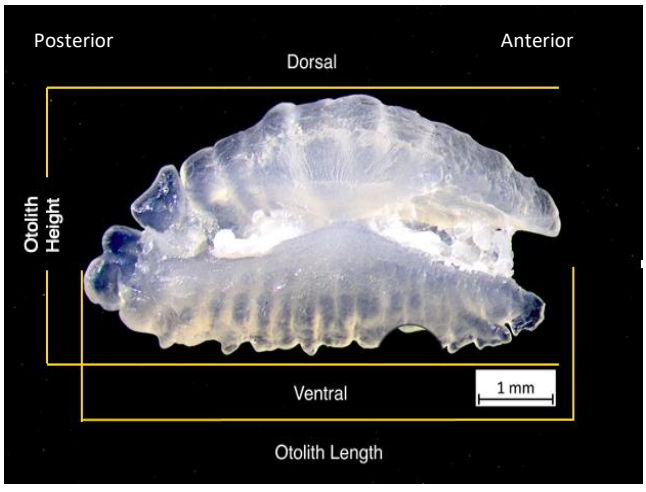

Figure 2. Sagitta otolith of *Cheilinus undulatus* (FL: 33.77 cm, FW: 680.39 g). Labels: Anterior (A), Posterior (P), Dorsal (D), Ventral (V), Otolith Length (OL), Otolith Height (OH)). Scale bar: 1 mm

Limitations

Due to the endangered status of *C. undulatus* and the strict collection permits required, specimen acquisition was limited. While the current dataset is essential for establishing a baseline for understanding morphological variability in *C. undulatus* populations in eastern Sabah, its spatial and temporal limitations must be acknowledged. The single-site, short-term sampling design restricts our ability to capture population heterogeneity and seasonal variation in growth or condition. Furthermore, reliance on fishery-dependent sampling may introduce selectivity bias, as hook-and-line techniques tend to favour size classes or behavioral types. Consequently, interpretations derived from the present study should be viewed as indicative rather than fully representative of the broader regional stock and are confined to the sampled population. The absence of age validation through annulus or increment counts remains a limitation as well. Consequently, interpretations of otolith growth trends were restricted to morphometric relationship rather than direct age estimation. However, data consistency across the measured parameters, the high regression fits, and narrow confidence intervals indicate strong reliability. These results are intended as foundational baseline data, supporting future studies on growth and population structure under broader spatial and temporal scales.

RESULTS AND DISCUSSION

Length-weight relationship and growth pattern

The current study showed that fish total length ranged from 27.51 to 103.88 cm (mean SD 35.28±11.72 cm) and body weight ranged from 330.24 to 19400.85 g. The LWR followed the model $W = 0.0139.L^{3.06}$ (a = 0.0139; b = 3.06). The linear regression analysis revealed a strong positive relationship between log-transformed total length (LOG10TL) and log-transformed fish weight (LOG10FW). As detailed in Table 1, the unstandardized coefficient (B) for LOG10TL was 3.062 (SE = 0.078, β = 0.988, t = 39.351, $p<0.001$), with a 95% confidence interval of [2.904, 3.219]. The intercept was estimated at -1.858 (SE = 0.121, t = -15.408, $p<0.001$), bounded by a 95% confidence interval of [-2.102, -1.614]. Collinearity diagnostics indicated no concerns, with tolerance and variance inflation factor values of 1.000 for the predictor. Residual diagnostics confirmed normality (Kolmogorov-Smirnov = 0.259; $p>0.05$), Durbin-Watson statistics for independence (1.836; values near 2.0) and visual inspections for heteroscedasticity (Residual plots showed no systematic patterns, confirming homoscedasticity). Although the slope (b = 3.06) was greater than 3.0, statistical findings suggest isometric growth patterns, supporting robust predictive reliability for the length-weight relationship model.

Complementing these statistical parameters, Figure 3 visually represents the length-weight relationship through a scatter plot of log10-transformed fish weight against log10-transformed total length, with individual data points clustered tightly around the fitted regression line (y = 3.0618x - 1.8581). The high coefficient of determination (r^2 = 0.9754) underscores the model's excellent fit, explaining approximately 97.5% of the variance in fish weight based on total length, and highlights the consistency of the observed isometric growth across the sampled specimens.

The length-frequency distribution of *C. undulatus* is unimodal, showing a marked concentration of individuals in the 26-28 cm size class, with an additional peak observed in the 102-104 cm class. The most frequently represented size class was 32-34 cm, comprising 12 individuals (29.27% of the specimens), which indicates a distinct peak in the population structure. The second most abundant class was 36-38 cm (n = 6; 14.63%), followed by the 30-32 cm and 34-36 cm classes (n = 5 each; 12.20%). The 28-30 cm and 38-40 cm classes each accounted for 9.76% (n = 4). Collectively, more than 80% of individuals were concentrated within the 28-40 cm range. In contrast, the least frequent classes, occurring at the distributional extremes (26-28, 40-42, 46-48, 48-50, and 102-104 cm), each contained only one individual (2.44%) (Figure 4).

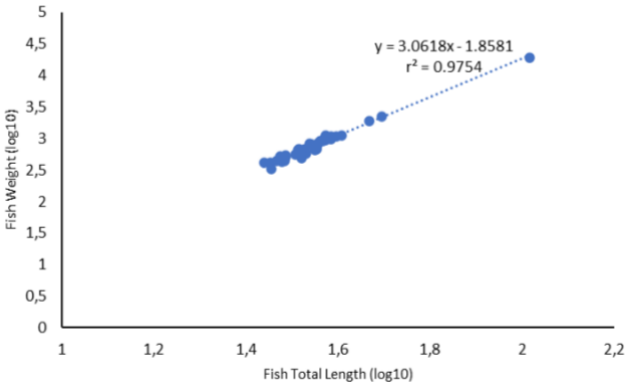

Figure 3. Scatter plot of fish total length (cm) against body weight of *Cheilinus undulatus*

Table 1. Regression coefficients for predicting LOG10FW from LOG10TL, including standard errors (SE), standardized coefficients (β), t-statistics, p-values, 95% confidence intervals (CI), and collinearity statistics (Tolerance and VIF). The model shows a strong, significant positive relationship with no multicollinearity issues

Predictor	B	SE	β	t	p	95% CI [Lower, Upper]	Tolerance	VIF
Constant	-1.858	0.121		-15.408	<0.001	[-2.102, -1.614]		
LOG10TL	3.062	0.078	0.988	39.351	<0.001	[2.904, 3.219]	1	1

Note: Dependent Variable: LOG10FW

Fish condition factor and size distribution

Findings on the Fulton condition factor (K) ranged from 1.319 to 2.089 across the entire size spectrum. Mean K-values remained consistent across size classes, with the lowest mean (1.64) recorded in the 32-34 cm class and the highest (1.88) in the 36-38 cm class. No linear or monotonic trend was detected between fish length and condition factor, although minor fluctuations were evident among size groups. Statistical testing confirmed that differences in mean K among classes were not significant ($p>0.05$). This interpretation is supported by the considerable overlap of error bars across adjacent size classes, indicating that the observed fluctuations are biologically negligible. Overall, fish ranging from 28 to 50 cm exhibited a stable physiological condition. Larger size classes (40-42, 46-48, 48-50, and 102-104 cm) lacked error bars due to single specimens. Notably, the largest class (102-104 cm; n = 1) showed a K value of 1.73, which was consistent with values observed in smaller classes (Figure 5).

With respect to size distribution, Figure 5 illustrates that the population structure was dominated by smaller to intermediate size classes. In contrast, larger individuals were rare in the sample, with only one specimen recorded in the largest size class (102-104 cm).

Relationship between otolith metrics and fish morphometry

Linear regression analyses demonstrated positive associations between otolith metrics and fish morphometry, with otolith weight (OW) showing the strongest correlations. As shown in Table 2, the coefficient (B) for LOG10OW ~ LOG10FL was 0.122 (SE = 0.010, $\beta = 0.886$, t = 11.902, $p<0.001$, 95% CI [0.101, 0.142]), with intercept -0.171 (SE = 0.016, t = -10.812, $p<0.001$, 95% CI [-0.204, -0.139]). Similarly, for LOG10OW ~ LOG10FW, B = 0.038 (SE = 0.003, $\beta = 0.875$, t = 11.284, $p<0.001$, 95% CI [0.031, 0.045]). Inter-otolith relations were robust, e.g., LOG10OW ~ LOG10OH (B = 0.025, SE = 0.003, $\beta = 0.830$, t = 9.278, $p<0.001$, 95% CI [0.020, 0.031]). Collinearity diagnostics revealed moderate interdependence (VIF 2.677-4.494), supporting model reliability. These findings validate otolith weight as a precise predictor of somatic size, with r^2 values up to 0.784, underscoring its utility in conservation contexts.

Residual diagnostics for the relationships between otolith metrics and fish morphometry confirmed the validity of the linear regression assumptions across all models. Normality of residuals was assessed using the Kolmogorov-Smirnov test with Lilliefors correction; for LOG10OL ~ LOG10FL, the test statistic was 0.138 (asymptotic p = 0.048, Monte Carlo p = 0.046 with 99% CI [0.041, 0.052]), indicating a marginal deviation, while other models showed non-significant results (likewise LOG10OH ~ LOG10FL: statistic 0.124, p = 0.121 with 99% CI [0.113, 0.130]; LOG10OW ~ LOG10FL: statistic 0.119, p = 0.157 with 99% CI [0.149, 0.165]), supporting normality in most cases. Heteroscedasticity was evaluated via scatterplots of standardized residuals against predicted values, revealing random distributions without funnel patterns or systematic trends, confirming homoscedasticity for all relationships (such as no clustering in LOG10OW ~ LOG10FW or inter-otolith models like LOG10OW ~ LOG10OH). Independence of residuals was verified using the Durbin-Watson statistic, with values ranging from 1.776 (LOG10OH ~ LOG10FW) to 2.012 (LOG10OL ~ LOG10FW), all near 2.0 and indicating no significant autocorrelation. These diagnostics affirm the reliability of the models, with any minor normality deviations in select cases not substantially impacting overall interpretations given the robustness of the associations (r^2 up to 0.784).

One left-side sagitta otolith examined from a specimen measuring 33.77 cm (FL) and 608.39 g (FW) displayed an elongate-oval morphology with irregular, undulating margins and a deep sulcus acusticus on the medial face. Its dimensions (~6.647 mm OL; 3.161 mm OH) correspond to the juvenile-subadult stage, during which otolith growth is linearly correlated to age and body size prior to sexual maturity (Mitcheson et al. 2019). The structure featured subtle rostrum and anterostrum projections bordering a shallow excisura (Figure 6), a configuration that supports age estimation through annulus counts in sectioned otoliths under transmitted light.

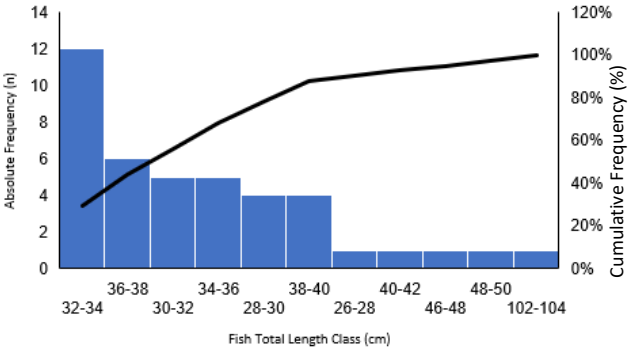

Figure 4. Length-frequency distribution of *Cheilinus undulatus* by 2-cm size classes (cm)

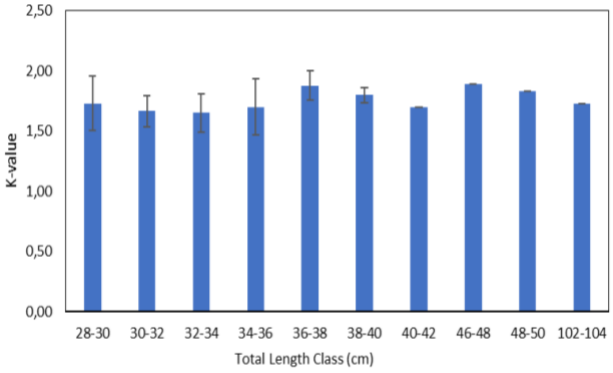

Figure 5. Condition Factor (K) of *Cheilinus undulatus* across 2-cm size classes

Table 2. Regression coefficients for otolith metrics and fish morphometry relationships, including SE, β, t-statistics, p-values, 95% CI, Tolerance, and VIF. Models show positive associations of varying strength, with moderate multicollinearity among otolith predictors but no severe issues

Relationship (Dependent ~ Predictor)	Predictor	B	SE	β	t	p	95% CI [Lower, Upper]	Tolerance	VIF
LOG10OL ~ LOG10FL	Constant	0.034	0.138		0.249	0.805	[-0.244, 0.313]		
	LOG10FL	0.503	0.089	0.672	5.662	<0.001	[0.323, 0.682]	1.000	1.000
LOG10OH ~ LOG10FL	Constant	-2.215	0.725		-3.055	0.004	[-3.682, -0.748]		
	LOG10FL	3.479	0.467	0.766	7.445	<0.001	[2.533, 4.424]	1.000	1.000
LOG10OW ~ LOG10FL	Constant	-0.171	0.016		-10.812	<0.001	[-0.204, -0.139]		
	LOG10FL	0.122	0.010	0.886	11.902	<0.001	[0.101, 0.142]	1.000	1.000
LOG10OH ~ LOG10OL	Constant	-0.717	0.487		-1.472	0.149	[-1.702, 0.268]		
	LOG10OL	4.785	0.597	0.789	8.015	<0.001	[3.577, 5.992]	1.000	1.000
LOG10OW ~ LOG10OL	Constant	-0.086	0.017		-4.960	<0.001	[-0.121, -0.051]		
	LOG10OL	0.127	0.021	0.690	5.958	<0.001	[0.084, 0.170]	1.000	1.000
LOG10OW ~ LOG10OH	Constant	-0.063	0.009		-7.242	<0.001	[-0.080, -0.045]		
	LOG10OH	0.025	0.003	0.830	9.278	<0.001	[0.020, 0.031]	1.000	1.000
LOG10OW ~ LOG10FW	Constant	-0.092	0.010		-9.487	<0.001	[-0.112, -0.073]		
	LOG10FW	1.167	0.134	0.813	8.734	<0.001	[0.897, 1.438]	1.000	1.000
Multicollinearity Assessment (LOG10FL ~ LOG10OL + LOG10OH + LOG10OW)	Constant	1.319	0.109		12.149	<0.001	[1.099, 1.539]		
	LOG10OL	0.138	0.164	0.103	0.840	0.406	[-0.195, 0.470]	0.374	2.677
	LOG10OH	0.007	0.035	0.030	0.186	0.853	[-0.065, 0.078]	0.223	4.494
	LOG10OW	5.749	0.985	0.790	5.839	<0.001	[3.754, 7.744]	0.308	3.243

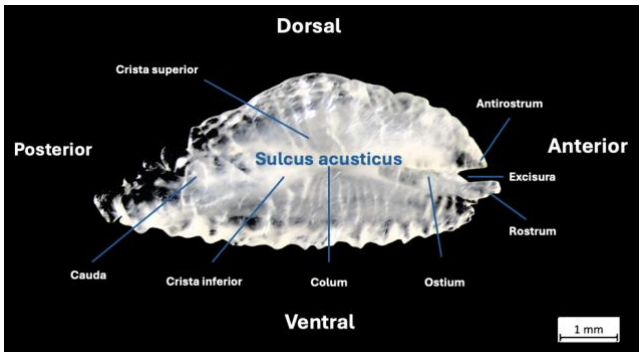

Figure 6. Anatomy of a sagitta otolith from *Cheilinus undulatus* (Fish Total Length (FL): 33.97 cm; Fish Weight (FW): 580.37 g; Scale bar: 1 mm; Otolith Length (OL): 7.15 mm; Otolith Height (OH): 3.09; Otolith Weight (OW): 0.014 g)

Discussion

Growth pattern and biological condition in wild and captive populations

The present findings suggest that growth patterns, condition factor, and the relationship between fish size and otolith dimensions serve as indicators for advancing biological research, supporting fisheries management, and guiding conservation efforts for endangered species (Brosset et al. 2023). The isometric growth pattern observed in *C. undulatus* from Eastern Sabah (b = 3.06, 95% CI [2.904, 3.219]), which body proportions remain constant throughout ontogeny, is consistent with patterns reported in other labrids exhibiting complex protogynous life histories. This proportionality aligns closely with isometric scaling documented in Ballan wrasse (*Labrus bergylta*; b = 3.04) and Peacock wrasse (*Symphodus tinca*; b = 3.01 in females), indicating that dimensional increases in length and weight occur at equivalent rates. This apparent stability suggests that the substantial size dimorphism and dynamic demography characteristic of large labrids are accommodated within proportional body scaling, preserving relative robustness and hydrodynamic efficiency throughout development. Importantly, the LWR observed in this study reflects growth patterns like those reported for other high-value reef fishes, including bluefish (*Pomatomus saltatrix*) and Sind sardinella (*Sardinella sindensis*), which exhibit (b) values ranging from 3.0 to 3.2. These findings underline the importance of interpreting the LWR within an ecological context, rather than perceiving it as a fixed species trait. Integrating ecological monitoring (e.g., prey availability, water quality and habitat complexity) with morphometric assessments provides a more comprehensive understanding of growth dynamics (Lewis et al. 2021). This insight is imperative for the formulation of adaptive management strategies that optimize wild population assessments and aquaculture practices.

However, it contradicts the growth patterns of some labrid species. The general trend observed across several other large labrid species (including the Hogfish (*Lachnolaimus*) and wrasses in the Philippines/Great Barrier Reef) is mostly negatively allometric (Aguilar-perera 2015; Lowe et al. 2022). This condition is possibly due to substantial size dimorphism and dynamic demography characteristic of large labrids, which are accommodated by changes in body proportions, rather than stability. Negative allometric trend (b<2.95) has also been documented in captive-reared *C. undulatus* maintained under Recirculated Aquaculture System (RAS) conditions (Tan et al. 2019). The marked contrast between wild and

captive populations underscores the pivotal role of environmental variables, such as foraging dynamics, spatial heterogeneity, and prey diversity, in promoting higher somatic growth in natural reefs (Asriyana et al. 2020; Dunic and Baum 2017). These attributes suggest limiting muscle development and energy allocation, thereby producing a lower b value (Austad et al. 2021; Magnaye et al. 2019).

The absence of sex differentiation in the present analysis is an acknowledged limitation given the protogynous hermaphroditic life history of the species. Sex change in this species typically occurs when individuals exceed a total length of 65-80 cm (Mitcheson et al. 2010) which point males exhibit distinct secondary sexual traits and potentially altered growth trajectories. Given the underrepresentation of larger individuals in the current sample, the dataset predominantly reflects juvenile and initial-phase females. This is likely to reduce the impact of sexual dimorphism on the length-weight and otolith-body regressions. Nonetheless, it is possible that sex-based variability may still contribute to subtle differences in morphometric scaling, particularly in the vicinity of the transition to terminal-phase males. To address this, future research should employ non-lethal sex identification techniques such as plasma steroid hormone profiling (Hara et al. 2016), ultrasonography (McGarvey et al. 2021) or analysis of external coloration (John et al. 2021), to differentiate between maturity stages. Incorporating these approaches is expectedly to enhance the accuracy of morphometric models and enable the evaluation of sex-related growth plasticity.

Condition factor and size distribution

The condition factor (K) is widely used in fisheries science to assess the health and energetic status of fish populations (Brosset et al. 2023; Engebretsen et al. 2024). In this study, Fulton's condition factor (K) was applied as a relative index of somatic well-being rather than an absolute indicator of health. As there are currently no species-specific reference baselines for *C. undulatus* in Malaysian waters, the interpretation of K-values was cautiously based on comparative data from other wrasses and coral reef fish of a similar trophic guild. The observed K range (1.3-2.1) indicates that the individuals exhibited balanced energy allocation between growth and maintenance, a characteristic typical of reef-dwelling carnivorous species inhabiting moderately productive coral ecosystems. The condition factor observed in this study is higher than that of other high-value demersal groupers and reef-associated fishes. For instance, the values are notably higher than those of the Goldblotch grouper (*Epinephelus costae*) (K = 1.002) and Saddled seabream (*Oblada melanura*) (K = 0.990) from the Eastern Mediterranean (Jisr et al. 2018). They are closely similar to those reported for the Dotdash goatfish (*Parupeneus barberinus*) and Common silver-buddy (*Gerres oyena*) from Youtefa Bay, Jayapura, Indonesia (Asriyana et al. 2020).

This comparative standing underscores that the population is not currently suffering from poor feeding conditions or environmental stress. However, the interpretation of K in *C. undulatus* should not fully rely on fixed thresholds, but rather on relative comparisons to baseline data derived from unexploited or well-managed populations. It is due to the K-value, which is highly correlated to species-specific and ecological or habitat contexts (Jisr et al. 2018). Recent research on the Eastern Sabah Ocean waters has experienced an increase in environmental threats, including illegal fishing, tourism, seaweed farming, sedimentation, and coral bleaching events (Bavoh et al. 2023). Further, the observed size distribution was notably skewed towards small and medium-sized individuals (28-40 cm). This is substantially below the known size-at-maturity for females (55 cm) (Choat et al. 2006) and males (84.5 cm) (Mitcheson et al. 2010), suggesting a population is presumed to be dominated by large juveniles. The marked underrepresentation of larger and mature individuals in the catch is a well-recognized indicator of size-selective fishing and is being observed in intensive exploited reef fisheries (Robinson et al. 2017; Wood et al. 2024). However, larger individuals of *C. undulatus* are discovered to occupy deeper reef slopes and impressive agility, therefore exhibit more cautious behavior, reducing their vulnerability to shallow artisanal capture (Ma et al. 2019). This condition should not be interpreted solely as evidence of selective fishing pressure. Given that sampling was conducted through artisanal fisheries, the observed structure likely reflects gear selectivity and habitat accessibility, rather than definitive population demography. Therefore, the apparent underrepresentation of large specimens may result from behavioral and habitat-related sampling bias rather than population-level depletion.

In addition, a relatively stable K-value may suggest good body condition across size groups, this pattern may not be directly linked to adaptive energy allocation or density compensation without supporting physiological or environmental data. Instead, the consistent K range is interpreted as indicative of stable body condition under the prevailing local habitat conditions during the sampling period. Nonetheless, while the population's health of observed specimens appeared acceptable on an individual basis, demographic structure and water parameter value, such as ORP, shows the signs of vulnerability, as a shrunken or truncated size distribution is an indication of fishing pressure that compromises stock resilience (Barnett et al. 2017; Wood et al. 2024). Therefore, it is evident that fishery management strategies should not be guided solely by this indicator. Future studies integrating fishery effort data, habitat mapping, and biochemical condition indicators (such as lipid profiles, gonadosomatic index) will provide a more definitive basis for evaluating fishing impacts and compensatory growth mechanism in this species (Zhu et al. 2020; Palma et al. 2023).

Integration of otolith metrics in growth and monitoring models

Linear regression analyses demonstrated positive associations between otolith metrics and fish morphometry, with otolith weight (OW) exhibiting the strongest correlations. This finding validates OW as a robust morphometric proxy for predicting total length in *C. undulatus*, with the coefficient (B) for LOG10OW ~ LOG10FL at 0.122 (SE =

0.010, β = 0.886, t = 11.902, p<0.001, 95% CI [0.101, 0.142]) and intercept at -0.171 (SE = 0.016, t = -10.812, p<0.001, 95% CI [-0.204, -0.139]). Comparable patterns have been documented in other teleosts, such as Sind sardinella (*S. sindensis*) and Flathead sillago (*S. panijus*), OW was similarly the most reliable predictor of fish length (Dehghani et al. 2015; Pradhan et al. 2022). Fish weight (FW) also exhibited a strong linear association with otolith OW (B = 0.038, SE = 0.003, β = 0.875, t = 11.284, p<0.001, 95% CI [0.031, 0.045]), reinforcing OW as the most informative predictor for both somatic size and body mass. Similar results were reported in Pama croaker (*Otolithoides pama*), with FW ~ OW and FL ~ OW yielding r^2 values of 0.81 and 0.84, respectively (Bhuiya and Siddique 2022). These outcomes support OW as a practical tool for assessing fish length and weight in field studies and morphometric research (Castro-Gutierrez et al. 2023).

Strong positive correlations were observed among otolith dimensions, with otolith length and height (OL ~ OH) showing the highest association, followed by moderately strong relations for OH ~ OW and OL ~ OW (such as LOG10OW ~ LOG10OH: B = 0.025, SE = 0.003, β = 0.830, t = 9.278, p<0.001, 95% CI [0.020, 0.031]). These patterns indicate proportional growth patterns within otolith morphometry. Analogous relationships have been noted in Brown comber (*Serranus hepatus*) and Two-banded seabream (*Diplodus vulgaris*), highlighting taxonomic consistency (Bilge et al. 2018; Khedher and Fatnassi 2018). The robust OL ~ OH correlation further suggests proportional otolith development during growth, consistent with evidence from Redcoat (*Sargocentron rubrum*), where otolith measurements linked closely to total length and condition factor (Kabakli and Erguden 2018).

Collectively, these results emphasize the utility of otolith morphometrics as reliable indicators of growth dynamics and physiological condition in reef-associated species. In addition, Britton and Blackburn (2014) demonstrated that integrating OW with fish length enhances age classification accuracy in flatfish, while OW offers a cost-effective alternative to otolith sectioning in resource-limited fisheries. Collinearity diagnostics indicated moderate interdependence (VIF 2.677-4.494), supporting model reliability without severe issues. However, the weaker FL ~ OL association (r^2 = 0.451) may stem from a narrower size range or sample limitations (Yildiz et al. 2018), with ontogenetic variability potentially contributing (Wei and Zhu 2022). While otolith analyses provide reliable estimates of age and growth rates, we acknowledge that they may not fully account for the complex influences of environmental variability; hence, we recommend that future research should integrate otolith-derived parameters with ecological monitoring and environmental profiling to further support a better understanding of growth patterns in *C. undulatus.*

Conservation implications

The current study provides first foundational dataset on the length-weight and otolith morphometric relationship of the endangered Napoleon wrasse (*C. undulatus*) in Eastern Sabah, contributing essential baseline information for future conservation and management assessments. Specifically, the observed growth pattern and strong correlations between otolith dimensions and fish size (r^2 up to 0.830) enable reliable proxies for estimating length and weight, facilitating non-invasive stock assessments through fishery-dependent data, such as landed catches. The findings presented herein may provide a scientific basis for the implementation of targeted management strategies. Such strategies may include the stricter enforcement of CITES Appendix II or local regulations, the establishment of marine protected areas in key habitats, such as Semporna area, and the introduction of minimum size limits aligned with maturity thresholds (>55 cm for females) to preserve spawning biomass and enhance population resilience (Choat et al. 2006; Robinson et al. 2017; Vincent et al. 2022). However, the scope of this study, due to some limitations, does not directly support demographic or stock-level management conclusions. This is suggested that the observed predominance of small and medium-sized individuals may suggest limited representation of older cohorts, demographic or stock level.

The present study has established a morphological and growth baseline for this endangered fish, thus addressing a significant gap in the existing body of empirical field data on the subject. The baseline provides a practical framework for the conservation effort of the species. In specific, the regression models and condition indices derived may also serve as non-lethal reference tools for the estimation of biomass or monitoring population condition in future ecological surveys. When implemented alongside the other fishery databases, such as underwater visual surveys and environmental DNA (eDNA), these metrics will enable rapid assessment of stock condition without the need for extensive destructive sampling (Lacoursiere-Roussel et al. 2016; Restiana et al. 2021). Thus, this study offers scientifically robust parameters that form the foundation for subsequent demographic modeling, spatial risk assessment and adaptive management strategies for *C. undulatus* across Indo-Pacific range. Moreover, these models hold considerable promise for the field of aquaculture, offering baseline growth parameters that can guide the refinement of rearing protocols in aquaculture systems.

The otolith characteristics confirm that the data originate from an immature stage, improving the suitability of growth models for protogynous hermaphrodites. Derived from the morphometric relationships in current study, otolith weight was found to strongly correlate with fish length (r^2 = 0.784) and weight (r^2 = 0.766). This underscored the utility of growth patterns in species such as *C. undulatus*. Such proxies enhance ecological assessments of population health, recruitment success and ecosystem productivity, supporting conservation strategies by reconstructing historical environmental exposure and predicting responses to human impact (Bavoh et al. 2023) and minimum capture sizes to safeguard juveniles and spawning adults (Mitcheson et al. 2019). This approach is essential to prevent recruitment overfishing and ensure the long-term sustainability and resilience of the *C. undulatus* stock (Rindorf et al. 2022). Engaging communities in conservation strategies through education, collaboration, and the consideration of their socio-economic needs may

foster trust and strengthen support for conservation initiatives. Incorporating sustainable fishing practices into these efforts can further demonstrate the tangible benefits of conservation to local communities, thereby enhancing cooperation and leading to more effective and long-term outcomes for *C. undulatus*.

Limitations and future directions

Whilst the present study provides valuable baseline information on the morphometric and otolith-body relationships of *C. undulatus* in Eastern Sabah, it is important to acknowledge several limitations that should be considered in guiding future research refinement. The sample size and spatial representativeness were constrained by the species' endangered status and limited capture permits. Although statistical analyses confirmed sufficient sample power for regression modelling, expanding sampling coverage across multiple reef habitats and monsoonal periods would strengthen the generalizability of the findings.

A further limitation concerns the absence of direct age validation and temporal environmental coverage. The present analyses were based on size-based morphometric groupings as opposed to increment-derived age estimation. It is recommended that future research incorporate validated ageing techniques, such as otolith thin-section microscopy or isotopic microchemistry, to establish a correlation between morphometric variation and chronological growth, as well as environmental history. Furthermore, environmental parameters were measured at a single time point; consequently, integrating seasonal and depth-stratified monitoring of temperature, salinity, oxygen, and light gradients will elucidate how habitat variability influences somatic and otolith growth patterns.

Notwithstanding the constraints, the present study provides a robust methodological framework for future integrative research. The integration of non-lethal biometric analyses with comprehensive environmental profiling and advanced molecular or imaging tools has the potential to significantly enhance our understanding of growth ecology and population resilience in *C. undulatus*. The incorporation of fishery-independent approaches, such as underwater visual censuses, baited remote underwater video (BRUVs), and environmental DNA (eDNA) surveys, would serve to further enhance ecological representativeness and validate population-level inferences. Addressing these aspects will enhance the ecological resolution of future studies and strengthen the evidence base required for adaptive conservation and management of this globally threatened reef species.

In conclusion, wild populations of the endangered Napoleon wrasse (*C. undulatus*) in Eastern Sabah, Malaysia, exhibit isometric growth patterns (b = 3.06, 95% CI [2.904, 3.219]), characterized by proportional increases in length and weight, alongside stable physiological condition (K = 1.319-2.089) and strong correlations between otolith metrics and somatic traits (r^2 = 0.451-0.784). The preponderance of juveniles (less than 40 cm) underscores the repercussions of selective overfishing, which endangers reproductive capacity and population recovery. The otolith-based morphometric insights presented here establish a critical baseline for stock assessments. This baseline is used to advocate for enhanced size-based regulations, habitat restoration, and community-driven conservation initiatives. These initiatives are used to mitigate exploitation pressures within the Coral Triangle. Despite being constrained by factors such as sample size and temporal scope, the findings underscore the efficacy of integrated metrics for the monitoring of protogynous species. It is imperative that future multidisciplinary research incorporating age validation, environmental dynamics, and fishery-independent surveys is conducted to inform adaptive management strategies, thereby ensuring the long-term viability of this ecologically pivotal reef predator amid escalating anthropogenic threats.

ACKNOWLEDGEMENTS

The authors would like to thank the staff and students in the Fish Hatchery of the Higher Institution Centre of Excellence, Borneo Marine Research Institute, Universiti Malaysia Sabah, Malaysia, for their unceasing support and technical assistance throughout the study. This paper was funded by the Higher Institution Centre of Excellence (HICoE) Research Grant Scheme (Approval Letter No. JPT(BKPI)1000/016/018/35(2), Grant Code HIC2402, provided by the Ministry of Higher Education, Malaysia.

REFERENCES

Abidin DAZ, Das SK, Abd Ghaffar M. 2019. Length-weight relationship, condition factors, and trophic level of Buffon's river-garfish *Zenarchopterus buffonis* from the coastal waters of Malaysia. Songklanakarin J Sci Technol 41 (5): 1162-1170.

Aguilar-perera A. 2015. Length - weight and length - length relationships of the hogfish, *Lachnolaimus maximus*, off the northern coast of the Yucatan Peninsula, Mexico. Gulf Caribb Res 26 (1): SC1-SC3. DOI: 10.18785/gcr.2601.02.

Arancibia H, Cisterna L, Sepúlveda A. 2021. Individual growth in Jack mackerel (*Trachurus murphyi*) of the Southeastern Pacific Ocean using sagitta otolith weight, daily rings, and annual rings. Gayana (Concepcion) 85: 95-102. DOI: 10.4067/s0717-65382021000100095.

Asriyana A, Irawati Nur, Halili H. 2020. Length-weight relationships and ponderal index of three reef fish (Teleostei: Labridae) off the Tanjung Tiram coast, Southeast Sulawesi, Indonesia. Biodiversitas 21 (4): 1279-1286. DOI: 10.13057/biodiv/d210402.

Austad B, Vollestad LA, Foldvik A. 2021. Frequency of vateritic otoliths and potential consequences for marine survival in hatchery-reared Atlantic salmon. J Fish Biol 98: 1401-1409. DOI: 10.1111/jfb.14683.

Barnett LA, Branch TA, Ranasinghe RA, Essington TE. 2017. Old-growth fishes become scarce under fishing. Curr Biol 27 (18): 2843-2848.e2. DOI: 10.1016/j.cub.2017.07.069.

Bavoh EM, Manjaji-Matsumoto BM, Mapait AJ, Ahmad MN, Lahum RA. 2023. Enhanced fish diversity following active coral reef restoration efforts in Tun Sakaran Marine Park, Sabah, Malaysian coral triangle. Trans Sci Technol 10 (4): 188-197.

Bhuiya A, Siddique MAM. 2022. Size frequency, length-weight relationships, condition factor, and relationships between fish size and otolith dimensions in the Pama croaker *Otolithoides pama* (Hamilton, 1822) from Lower Meghna River Estuary, Bangladesh. Lakes Reserv Res Manag 27 (3): e12418. DOI: 10.1111/lre.12418.

Bilge G, Yapıcı S, Halit FM. 2018. Relationships between fish and otolith dimensions for *Serranus hepatus* (Linnaeus, 1758) from the Southern Aegean Sea. Nat Eng Sci 3: 128-132. DOI: 10.28978/nesciences.424655.

Britton JR, Blackburn R. 2014. Application and utility of using otolith weights in the ageing of three flatfish species. Fish Res 154: 147-151. DOI: 10.1016/j.fishres.2014.02.005.

Brosset P, Averty A, Mathieu-Resuge M, Schull Q, Soudant P, Lebigre C. 2023. Fish morphometric body condition indices reflect energy reserves, but other physiological processes matter. Ecol Indic 154 (8): 110860. DOI: 10.1016/j.ecolind.2023.110860.

Castro-Gutiérrez J, Madera-Santana S, Rodríguez-García C, Domínguez-Bustos ÁR, Sarmiento-Carbajal J, Gonçalves-Neto JB, Cabrera-Castro R. 2023. Exploring morphometric frontiers: A comprehensive study of otolith growth patterns in brown comber (*Serranus hepatus*) (Linnaeus, 1758). J Fish Biol 103: 1374-1381. DOI: 10.1111/jfb.15544.

Choat JH, Davies CR, Ackerman JL, Mapstone BD. 2006. Age structure and growth in a large teleost, *Cheilinus undulatus*, with a review of size distribution in labrid fishes. Mar Ecol Prog Ser 318: 237-246. DOI: 10.3354/meps318237.

De Souza GM, Tubino RD, Monteiro-Neto C, Costa MR. 2019. Relationships between fish and otolith dimensions of *Pomatomus saltatrix* (Linnaeus, 1766) (Perciformes: Pomatomidae) in Southeastern Brazil. Neotrop Ichthyol 17 (1): 1-8. DOI: 10.1590/1982-0224-20180032.

Dehghani M, Kamrani E, Salarpouri A, Kamali E. 2015. Relationship between fish length and otolith dimensions (length, width) and otolith weight of *Sardinella sindensis*, as an index for environmental studies, persian gulf, Iran. J Fish Livest Prod 03 (134): 2. DOI: 10.4172/2332-2608.1000134.

Dunic JC, Baum JK. 2017. Size structuring and allometric scaling relationships in coral reef fishes. J Anim Ecol 86 (3): 577-589. DOI: 10.1111/1365-2656.12637.

Engebretsen S, Aldrin M, Lunde L, Austad M, Rafoss T, Danielsen OR, Lindhom A, Boissonnot L, Jansen PA. 2024. Condition factor tailored to lumpfish (*Cyclopterus lumpus*) used as a cleaner fish in salmonid farms. Aquac Rep 35: 101996. DOI: 10.1016/j.aqrep.2024.101996.

Froese R. 2006. Cube law, condition factor and weight-length relationships: History, meta-analysis and recommendations. J Appl Ichthyol 22 (4): 241-253. DOI: 10.1111/j.1439-0426.2006.00805.x.

Hara A, Hiramatsu N, Fujita T. 2016. Vitellogenesis and choriogenesis in fishes. Fish Sci 82 (2): 187-202. DOI: 10.1007/s12562-015-0957-5.

Jisr N, Younes G, Sukhn C, El-Dakdouki MH. 2018. Length-weight relationships and relative condition factor of fish inhabiting the marine area of the Eastern Mediterranean city, Tripoli-Lebanon. Egypt J Aquat Res 44 (4): 299-305. DOI: 10.1016/j.ejar.2018.11.004.

John L, Rick IP, Vitt S, Thunken T. 2021. Body coloration as a dynamic signal during intrasexual communication in a cichlid fish. BMC Zool 6 (1): 1-13. DOI: 10.1186/s40850-021-00075-9.

Kabakli F, Erguden D. 2018. Relationships between fish length and otolith dimensions of redcoat, *Sargocentron rubrum* (Forsskal, 1775) in the southeastern Mediterranean Sea, Turkey. Turk J Maritime Mar Sci 4 (2): 156-162.

Khedher M, Fatnassi M. 2018. Relationships between fish length and otolith size of *Diplodus vulgaris* from Boughrara and El Bibane Lagoons (southeastern Tunisia). Res Rev J Zool Sci 6: 43-50.

Lacoursiere-Roussel A, Cote G, Leclerc V, Bernatchez L. 2016. Quantifying relative fish abundance with eDNA: A promising tool for fisheries management. J Appl Ecol 53 (4): 1148-1157. DOI: 10.1111/1365-2664.12598.

Lewis LS, Denney C, Willmes M, Xieu W, Fichman RA, Zhao F, Hammock BG, Schultz A, Fangue N, Hobbs JA. 2021. Otolith-based approaches indicate strong effects of environmental variation on growth of a Critically Endangered estuarine fish. Mar Ecol Prog Ser 676: 37-56. DOI: 10.3354/meps13848.

Liu M, Sadovy Y. 2011. Forehead morphology of the humphead wrasse *Cheilinus undulatus* (Perciformes: Labridae) in relation to body size forehead morphology of the humphead wrasse *Cheilinus undulatus* (Perciformes : Labridae) in relation to body size. Ichthyol Herpetol 2011 (2): 315-318. DOI: 10.2307/41261882.

Lowe JR, Russ GR, Bucol AA, Abesamis RA, Stockwell BL, Choat JH. 2022. Patterns of biogeographic and regional life-history trait variation in four large-bodied tropical wrasses. Mar Biol 169: 113. DOI: 10.1007/s00227-022-04098-9.

Magnaye M, Rideout RM, Davoren G. 2019. Irregular growth patterns in the otoliths of a short-lived forage fish do not reliably indicate reproductive history. Fish Res 218 (5): 120-126. DOI: 10.1016/j.fishres.2019.05.007.

Ma KY, Colin PL, Sadovy de Mitcheson Y, Dawson MN. 2019. Phylogeography and conservation biogeography of the Humphead Wrasse, *Cheilinus undulatus*. Front Biogeogr 11 (2): e42697. DOI: 10.21425/f5fbg42697.

McGarvey LM, Ilgen JE, Guy CS, McLellan JG, Webb MA. 2021. Gonad size measured by ultrasound to assign stage of maturity in Burbot. J Fish Wildl Manag 12 (1): 241-249. DOI: 10.3996/jfwm-20-082.

Mitcheson YSD, Liu M, Suharti SR. 2010. Gonadal development in a giant threatened reef fish, the humphead wrasse (*Cheilinus undulatus*), and its relationship to international trade. J Fish Biol 77 (3): 706-718. DOI: 10.1111/j.1095-8649.2010.02714.x.

Mitcheson YSD, Suharti SR, Colin PL. 2019. Quantifying the rare: baselines for the endangered Napoleon Wrasse, *Cheilinus undulatus*, and implications for conservation. Aquat Conserv 29 (8): 1285-1301. DOI: 10.1002/aqc.3124.

Nanola CL, Paradela MAC, Songco AM. 2021. First report on the density and size frequency distribution of the Napoleon wrasse, *Cheilinus undulatus*, in the Tubbataha Reefs Natural Park, Philippines. Philipp J Sci 150 (1): 209-221. DOI: 10.56899/150.01.18.

Palma PA, Lwin SS, Jimenez-Fernandez E. 2023. Insights into the early gonad development of the protogynous ballan wrasse (*Labrus bergylta*). Aquac Rep 33: 101857. DOI: 10.1016/j.aqrep.2023.101857.

Pradhan SK, Sri Hari M, Roul SK, Ghosh S, Jaiswar AK, Nayak BB, Bhusan S. 2022. Relationship between fish and otolith dimensions of flathead sillago *Sillaginopsis panijus* (Hamilton, 1822) (Perciformes: Sillaginidae) in the north-western Bay of Bengal. Indian J Fish 69 (3): 155-160. DOI: 10.21077/ijf.2022.69.3.102825-19.

Prianto E, Puspasari R, Oktaviani D, Sulaiman PS, Anggawangsa RF. 2019. Pemanfaatan ikan Napoleon (*Cheilinus undulatus*) melalui sistem perikanan budidaya di Kabupaten Natuna. J Kebijak Perikan Indones 11 (2): 101. DOI: 10.15578/jkpi.11.2.2019.101-111. [Indonesian]

Restiana E, Gelis E, Kamal MM. 2021. Environmental biomonitoring of reef fish community structure with eDNA metabarcoding in the Coral Triangle. Environ Biol Fishes 104 (8): 887-903. DOI: 10.1007/s10641-021-01118-3.

Rindorf A, van Deurs M, Howell D, Andonegi E, Berger A, Bogstad B, Cadigan N, Elvarsson BÞ, Hintzen N, Savina Roland M, Taylor M. 2022. Strength and consistency of density dependence in marine fish productivity. Fish Fish 23 (4): 812-828. DOI: 10.1111/faf.12650.

Robinson JP, Williams ID, Edwards AM, McPherson J, Yeager L, Vigliola L, Brainard RE, Baum JK. 2017. Fishing degrades the size structure of coral reef fish communities. Glob Change Biol 23 (3): 1009-1022. DOI: 10.1111/gcb.13482.

Roe P, Hashim AS, Evans V, de Mitcheson YS. 2022. Status of Napoleon wrasse in Laamu Atoll, Maldives, after three decades of protection. Endangered Species Res 49: 135-144. DOI: 10.3354/esr01210.

Syam AR, Mujiyanto, Indriatmoko. 2020. Sustainable aquaculture of a protected species: The case of juvenile humphead wrasse (*Cheilinus undulatus*) around the Anambas Islands. IOP Conf Ser Earth Environ Sci 521 (1): 012014. DOI: 10.1088/1755-1315/521/1/012014.

Tan BL, Ching FF, Senoo S. 2019. Body size and morphological characteristics in sex determination of humphead wrasse (*Cheilinus undulatus*) in captivity. J Phys Conf Ser 1358 (1): 012010. DOI: 10.1088/1742-6596/1358/1/012010.

Vincent ACJ, Foster S, Fowler S. 2022. Implementing CITES Appendix II listings for marine fishes: A novel framework and a constructive analysis. Fish Cent Res Rep 30 (3): 189. DOI: 10.14288/1.0421719.

Wei X, Zhu G. 2022. Shape and ontogenetic changes in otolith of the ocellated icefish (*Chionodraco rastrospinosus*) from the Bransfield Strait, Antarctic. Zoology 153: 126025. DOI: 10.1016/j.zool.2022.126025.

Wood MV, Carvalho FM, Castello L. 2024. Fishing shrinks the size structure of exploited coral reef fishes in Brazil. Fish Res 275: 107029. DOI: 10.1016/j.fishres.2024.107029.

Yildiz T, Zengin M, Uzer U, Akpinar IO, Karakulak FS. 2018. Length-weight relationships for 24 fish species collected from the western Black Sea (Turkey). Cahiers de Biologie Marine 59: 159-165. DOI: 10.21411/CBM.A.39436D05.

Zhu Y, Wu J, Leng X, Du H, Wu J, He S, Luo J, Liang X, Liu H, Wei Q, Tan Q. 2020. Metabolomics and gene expressions revealed the metabolic changes of lipid and amino acids and the related energetic mechanism in response to ovary development of Chinese sturgeon (*Acipenser sinensis*). PLoS One 15 (6): e0235043. DOI: 10.1371/journal.pone.0235043.